

# Interferometric Scattering Microscopy to Characterize Nanometric Objects and Subcellular Structures: Towards Fast 3D Imaging at Nanoscale.

I.-B. Lee<sup>1,2</sup>, J.-S. Park<sup>1</sup>, H.-M. Moon<sup>1,2</sup>, K. Zambochova<sup>1,3</sup>, K.-H. Kim<sup>1,2</sup>, J.-H. Joo<sup>1,4</sup>, J.-S. Ryu<sup>5</sup>, S.-Y. Kong<sup>6</sup>, **S.-C. Hong<sup>1,2\*</sup>**, and M. Cho<sup>1,4\*</sup>

<sup>1</sup>Center for Molecular Spectroscopy and Dynamics, Institute for Basic Science (IBS), Seoul 02841, Korea.

<sup>2</sup>Department of Physics, Korea University, Seoul 02841, Korea

<sup>3</sup>Department of Natural Sciences, Faculty of Biomedical Engineering, Czech Technical University in Prague, Kladno 27201, Czech Republic

<sup>4</sup>Department of Chemistry, Korea University, Seoul 02841, Korea

<sup>5</sup>Center for Breast Cancer, National Cancer Center, Goyang, 10408, Korea

<sup>6</sup>Division of Translational Science, National Cancer Center, Goyang, 10408, Korea

\*email: hongsc@korea.ac.kr and mcho@korea.ac.kr

IBS 기초과학연구원  
Institute for Basic Science

KOREA UNIVERSITY  
고려대학교

CMSD  
Center for Molecular Spectroscopy and Dynamics, IBS-Korea University

## Abstract

It is of great interest to visualize nano-scale objects in bioscience. Fluorescence microscopy, most powerful to date, bears limitations in measurement time, time resolution, and sample preparation. To circumvent such problems, a new scattering-based method named iSCAT (interferometric scattering microscopy) has been recently introduced. Since this technique relies on scattering signal from a target particle such as gold nanoparticle (AuNP) and detects the interference of the signal with a constant reference, it is not subject to the aforementioned limitations: theoretically unlimited SNR to improve time resolution, practically unlimited measurement time for localized scatterers, and lack of photo-blinking and photo-bleaching. Here, we report our recent achievements: First, we utilized polarized scattering from an anisotropic scatterer to characterize the position and orientation of nanorods. From this new scheme (psiSCAT), we capture the orientation of gold nanorods (AuNR) without sacrificing the bright-field image of the entire view-field, in contrast to dark-field imaging [1]. Second, we successfully track the position of nanoparticles along the axial dimension and image the sample at different depths by adopting the remote-focusing (RF) technique. Our RF-iSCAT approach significantly expands the strength and utility of iSCAT [2]. Lastly, we show our iSCAT imaging of biological cells and multi-protein focal adhesion complexes. The iSCAT technique enables us to visualize subcellular structures with remarkable spatial, temporal details and contrast even without labeling [3]. The iSCAT technique would be an indispensable tool in visualizing the nanoscopic biological world.

## Principle of iSCAT detection

$$I_{\text{detection}} = |E_i|^2 \{r^2 + s^2 + 2rs \cos(\Delta\phi)\} \text{ where } \Delta\phi = \phi_r - \phi_s$$

$$I_{\text{ratio}} = \frac{I_{\text{detection}} - I_{\text{background}}}{I_{\text{background}}} = \frac{2}{r^2} + 2 \frac{s}{r} \cos(\Delta\phi)$$

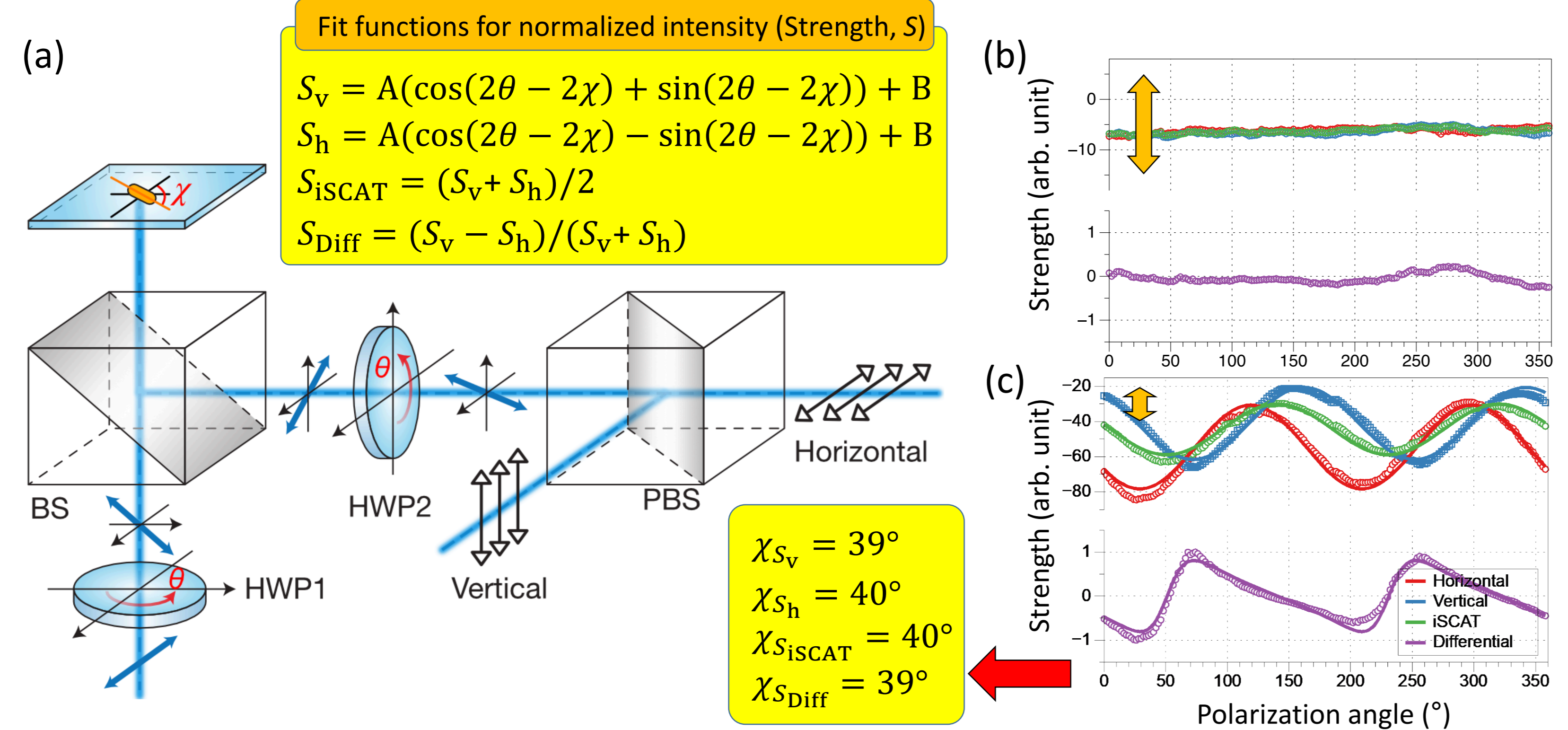
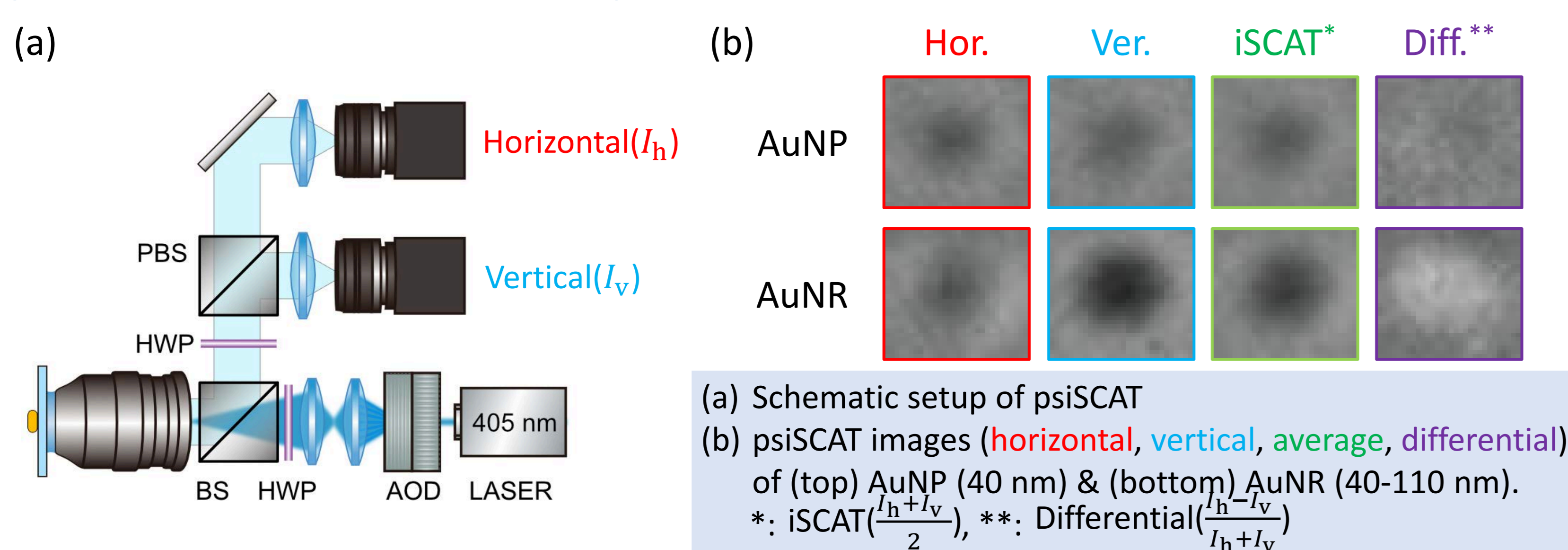
Scattering cross-section ( $\sigma$ )  
 $\sigma = |s|^2 \propto \epsilon_m^2 \pi \frac{D^6}{4\lambda^4} \left| \frac{\epsilon_p - \epsilon_m}{\epsilon_p + 2\epsilon_m} \right|^2$

The iSCAT signal varies with  $D^3$  while the dark-field signal (pure scattering) with  $D^6$ : the weaker size dependence of iSCAT permits a wider dynamic range of detectable size.

Scattering cross-section ( $\sigma$ )

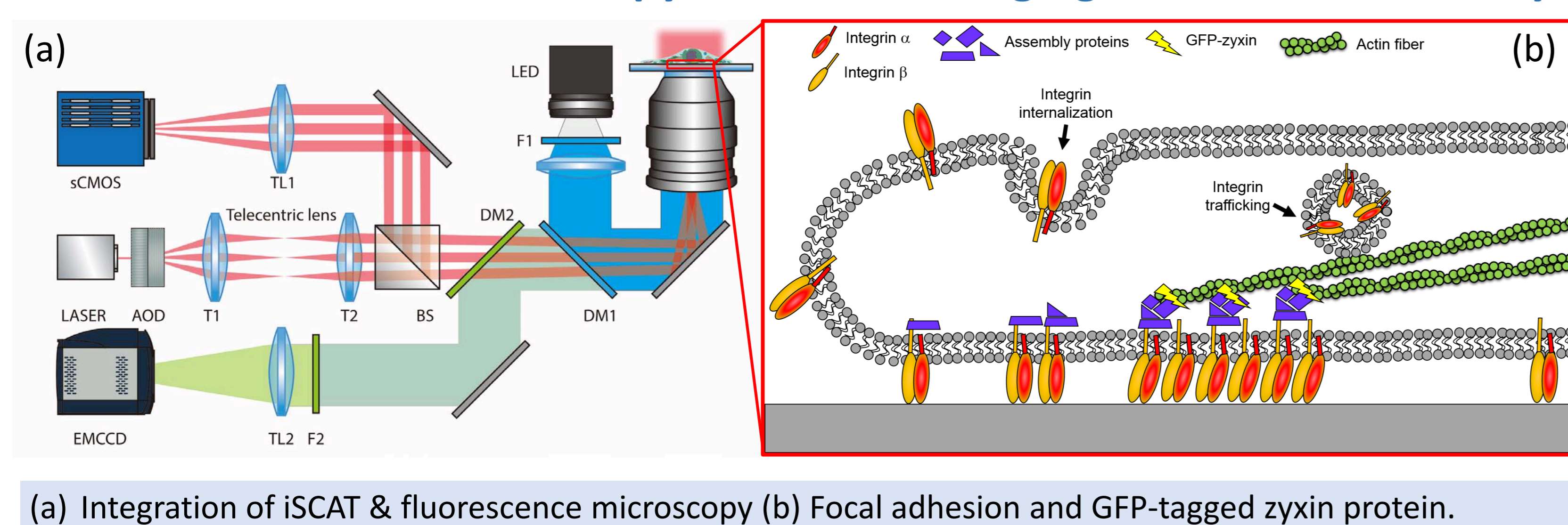
The iSCAT signal varies with  $D^3$  while the dark-field signal (pure scattering) with  $D^6$ : the weaker size dependence of iSCAT permits a wider dynamic range of detectable size.

## polarization-selective iSCAT (psiSCAT)



(a) Schematic view of psiSCAT detection. Input polarization ( $\theta$ ) is rotated by HWP1 and output polarization is adjusted by  $\theta$  by HWP2. Polarization selective detection by PBS provides the orientation of nanorod ( $\chi$ ). (Inset: angle-dependence of various modes of strength) (b, c) Polarization-dependence of strengths from AuNP (b) and AuNR (c). Orange arrows indicate the same scale ( $\Delta\text{Strength} = 20$ ) in (b) and (c).

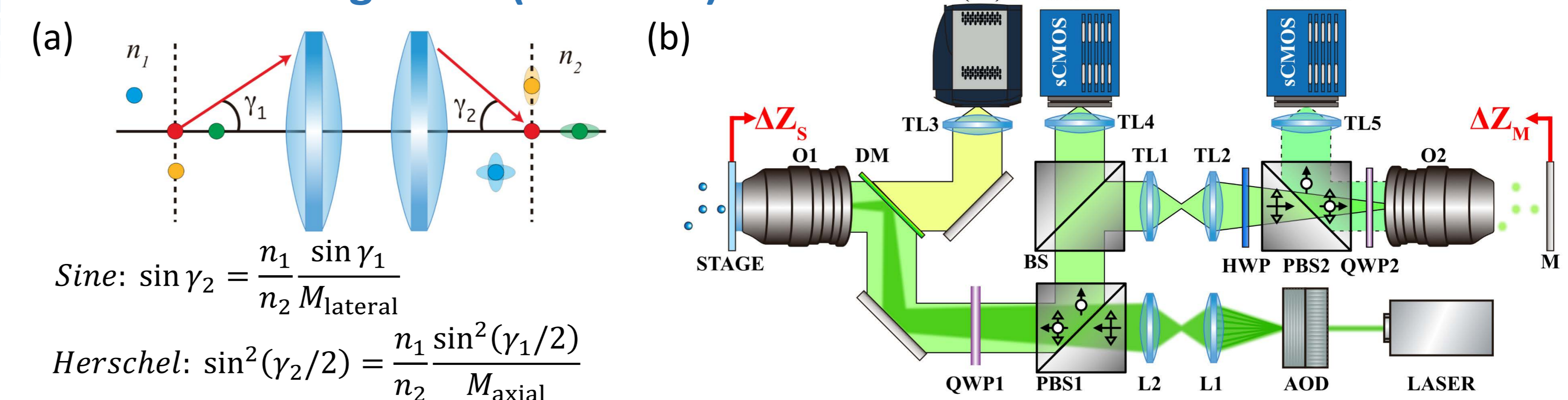
## iSCAT + fluorescence microscopy for live cell imaging: focal adhesion study



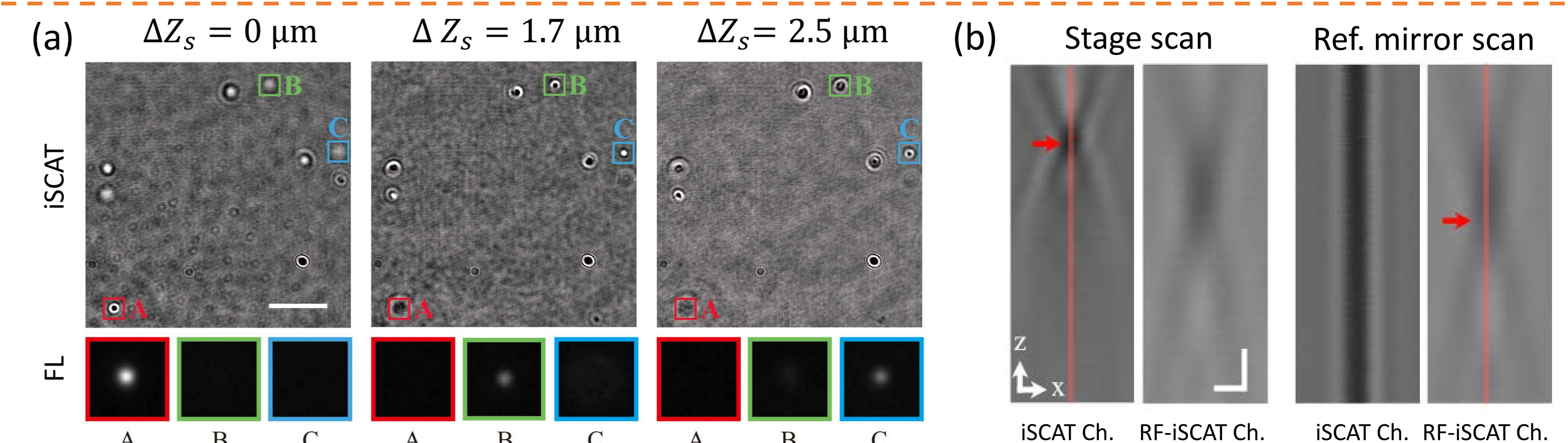
## Conclusions

- We developed several novel techniques in iSCAT microscopy:
  - The psiSCAT technique can determine the orientation as well as the position of nanorods.
  - The RF-iSCAT technique permits fast, vibration-free, 3D tracking of nano-objects.
- We succeeded in visualizing live cells with iSCAT combined with fluorescence microscopy:
  - The FM-combined iSCAT can image organelles & multi-protein complexes selectively with great temporal and spatial details. It can track them for unlimited measurement time.

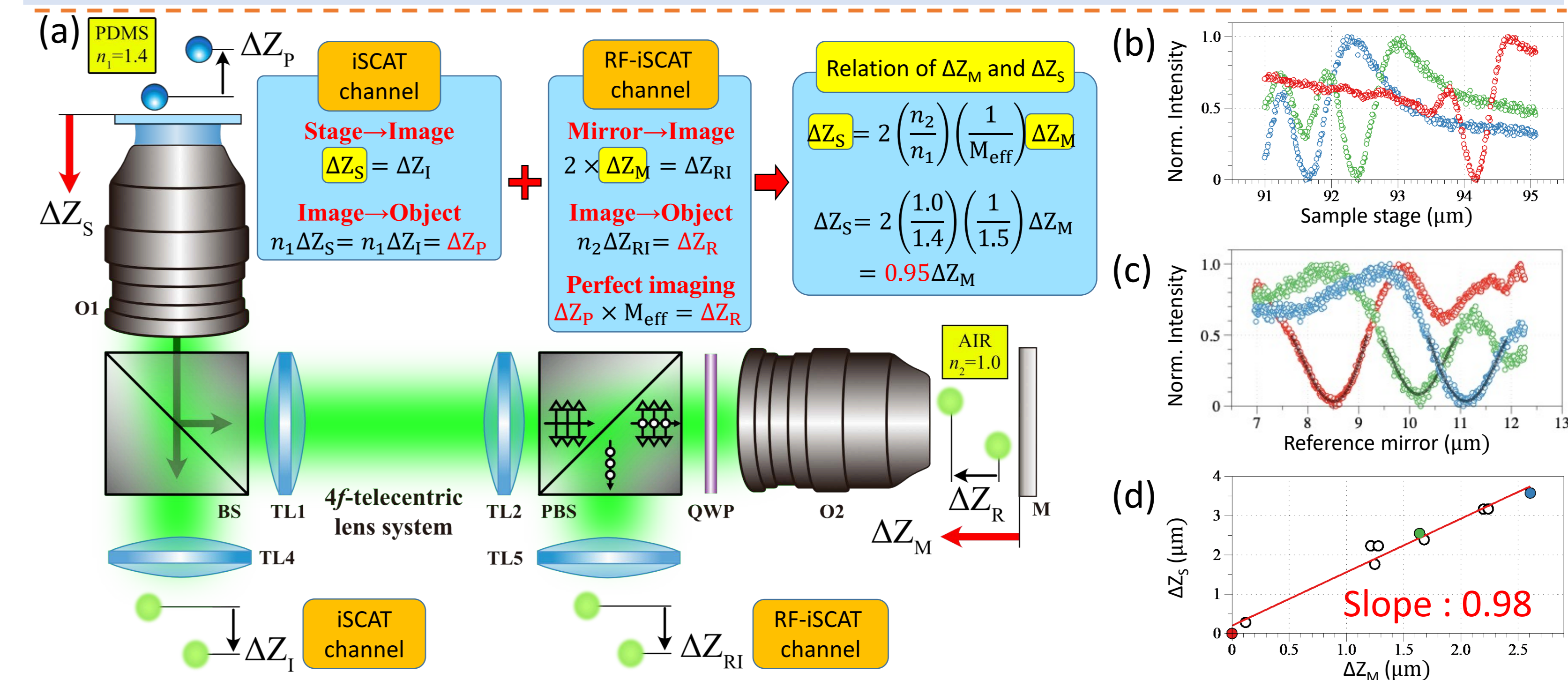
## Remote Focusing iSCAT (RF-iSCAT)



(a) Perfect imaging and optical aberrations: conditions for lateral (Sine) and axial (Herschel) perfect imaging. (b) Schematic setup of RF-iSCAT.

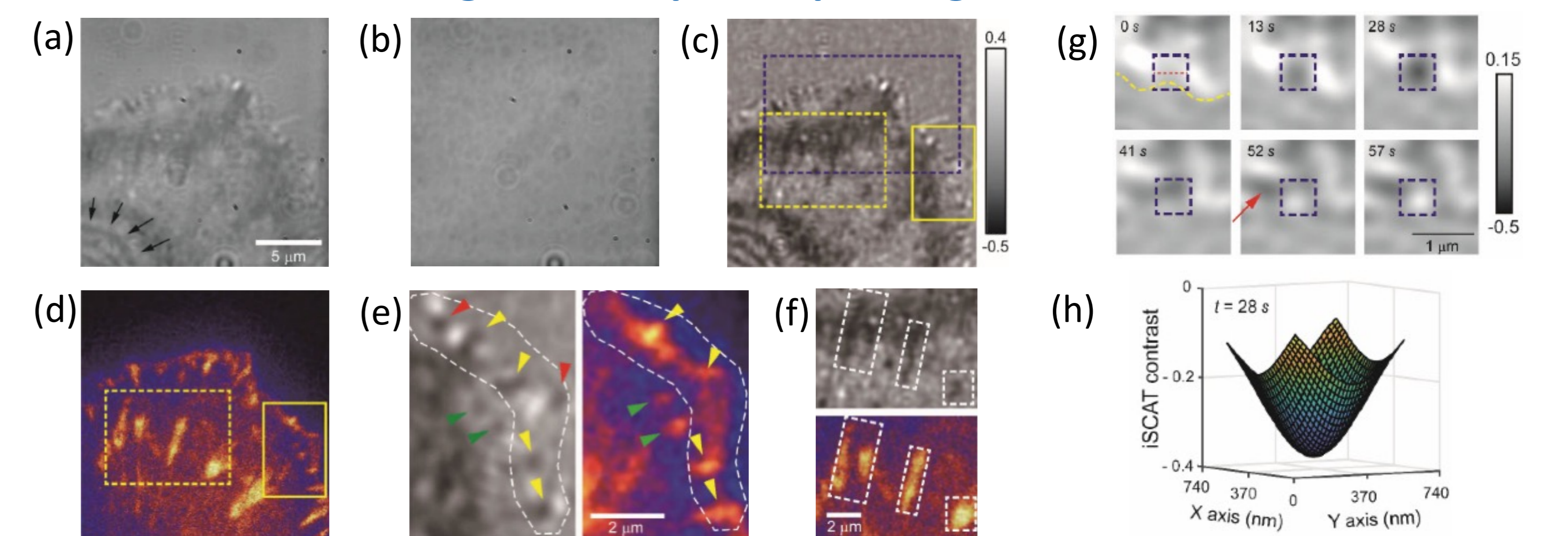


(a) Representative iSCAT (top) and fluorescence images (bottom) of fluorescent PS beads (A, B, & C; Dia. = 0.2  $\mu\text{m}$ ) within a PDMS film at different depths ( $\Delta Z_s$ ). Scale bar: 5  $\mu\text{m}$ . (b) Stacked intensity profiles of bead A acquired by translating either sample stage (left) or reference mirror (right) and measured in both iSCAT and RF-iSCAT channels. Red arrows mark the z-position of bead A. Scale bar: 0.5  $\mu\text{m}$ .



(a) Schematic diagram of key optics for RF-iSCAT and definitions of and relations between various z displacements. (b, c) Normalized intensity variations of the center of bead (A: red, B: green, C: blue) with respect to the position of sample stage (b) or reference mirror (c). (d) Linearity and near identity between the stage height and the mirror position for focusing of beads (each point represents a different bead).

## Fast label-free tracking of FA & specific probing of GFP-labeled FA in U2OS



(a) Raw iSCAT image, (b) mean background image of 1,000 consecutive frames from a cell-free area, (c) ratiometric iSCAT image obtained from the ratio of (a) to (b), (d) complementary fluorescent image showing zyxin-rich regions, (e) magnified iSCAT image (area boxed by yellow solid line in (c)) showing the existence of adhesions in the cell boundary (left) and its complementary fluorescent image (right), (f) magnified iSCAT image (area boxed by yellow dotted line in (c)) showing the structure of mature FAs (upper) and corresponding fluorescence image (lower). (g) Sequential images showing a whole life span of a single nascent adhesion, (h) Gaussian fit to define the center of a nascent adhesion.

## References

- [1] I.-B. Lee, H.-M. Moon, J.-H. Joo, K.-H. Kim, S.-C. Hong, and M. Cho, *ACS Photonics*, **5**, 797 (2017).
- [2] I.-B. Lee, H.-M. Moon, J.-S. Park, K. Zambochova, S.-C. Hong, and M. Cho, *Optics Letters*, *under revision*.
- [3] J.-S. Park, I.-B. Lee, H.-M. Moon, J.-H. Joo, K.-H. Kim, S.-C. Hong, and M. Cho, *Chem. Sci.*, **9**, 2690 (2018). J.-S. Park, I.-B. Lee, H.-M. Moon, J.-S. Ryu, S.-Y. Kong, S.-C. Hong, and M. Cho, *to be resubmitted*.

## Acknowledgement

This work was supported by IBS-R023-D1 and NRF-2019R1H1A2077487.